Study of baryonic resonances and ρ meson production in the reaction $pp \rightarrow pp\pi^+\pi^-$ at 3.5 GeV with HADES

Amel Belounnas[1,3,*]
for the HADES collaboration

[1]Institut de Physique Nucléaire d'Orsay, CNRS-IN2P3, Univ. Paris Sud, Univ. Paris-Saclay, 91406 Orsay Cedex, France.

Abstract. The High Acceptance Di-Electron Spectrometer (HADES) installed at GSI in Darmstadt and designed to investigate dielectron production in heavy-ion collisions in the range of kinetic beam energies 1-3 A GeV is also an excellent detector for charged hadron detection. We discuss the analysis of the $pp \rightarrow pp\pi^+\pi^-$ channel at an incident energy of 3.5 GeV, using results from pp→ppπ^0, pp→pnπ^+ and $pp \rightarrow pK\Lambda$ measured at the same energy by HADES. A consistent description of the differential cross sections as a function of the invariant mass and the production angles is achieved by a simple resonance model taking into account the single and the double excitation of baryonic resonances with masses up to 1.9 GeV. The contributions can be quantified and confronted to the inputs of transport models or to the predictions of dedicated models for nucleon-nucleon reactions. In addition, using specific kinematical cuts, the total production cross section and the angular distribution of the ρ meson have been also extracted. As both baryon resonances and the ρ meson are important sources of di-electrons, these results will provide valuable constraints for the interpretation of the dielectron spectra measured by the HADES collaboration.

1 Introduction

The High Acceptance DiEelectron Spectrometer (HADES) [1] installed at GSI in Darmstadt was built to investigate dielectron production in order to study the hot and dense hadronic medium produced in heavy-ion collisions in the 1-2 AGeV energy range. Proton- or pion-nucleus reactions are also investigated to probe cold nuclear matter. Moreover, the experimental programme also comprises elementary reactions (pp, quasi-free np, and πp) to study more selectively the different dilepton sources (see P. Salabura's report at this conference [2] for an overview). In particular, baryonic resonances are important sources of dileptons through two mechanisms: their Dalitz decays (e.g. $\Delta/\mathrm{N}^\star \rightarrow N\mathrm{e}^+\mathrm{e}^-$) and the mesonic decays with subsequent dilepton decay ($\pi^0 \rightarrow \gamma\mathrm{e}^+\mathrm{e}^-$, $\eta \rightarrow \gamma\mathrm{e}^+\mathrm{e}^-$, $\omega/\rho \rightarrow \mathrm{e}^+\mathrm{e}^-$). According to Vector Meson Dominance [3], electromagnetic transitions between hadrons are mediated by vector mesons, which strongly connects the Dalitz decay of baryons to their coupling to vector mesons. The ρ meson is expected to play a big role, over a broad kinematic region, due to its large width and strong coupling to baryons. The possibility to measure simultaneously with the HADES detector meson and di-electron production is therefore a great advantage. In this way, constraints on reaction mechanisms, and in particular on the role of intermediary baryon resonances, obtained by the study of the meson production channels can indeed be used for the interpretation of the dielectron production.

This motivated previous studies of the HADES collaboration in the 1π, η, $K\Lambda$ and $K\Sigma$ production channels in pp reactions from 1.25 to 3.5 GeV [4–7]. The 2π production channel offers the additional possibility to study the double baryon excitation, and, at high enough energies, ρ meson production. A previous study of the 2π production by the HADES collaboration in the $pn \rightarrow pn\,\pi^+\pi^-$ channel at 1.25 GeV [8] showed strong contributions of both the double $\Delta(1232)$ and of the N(1440) excitation. This contribution focuses on the analysis of the $pp \rightarrow pp\,\pi^+\pi^-$ reaction at 3.5 GeV. At such high energies, one can also expect the exctation of higher resonances. Therefore, the reaction is well suited to study the single and double excitation of many baryon resonances the production of the ρ meson, either directly or via the decay of baryon resonances.

2 Previous HADES studies

HADES (High Acceptance Di-Electron Spectrometer) was designed for the detection of $\mathrm{e}^+\mathrm{e}^-$ pairs, but it is also an excellent detector for charged hadron detection. It consists of six identical sectors covering polar angles between 18° and 85° with respect to the beam axis. A hadron blind RICH detector is used for the identification of e^+ and e^-. The momentum vectors of produced particles are reconstructed by means of the four drift chambers (MDC), two placed before and two placed behind the magnetic field region provided by six coils of a super-conducting toroid. In the detector configuration used for this experiment, time-of-flight information was given by two time-of-flight walls

*e-mail: ramstein@ipno.in2p3.fr

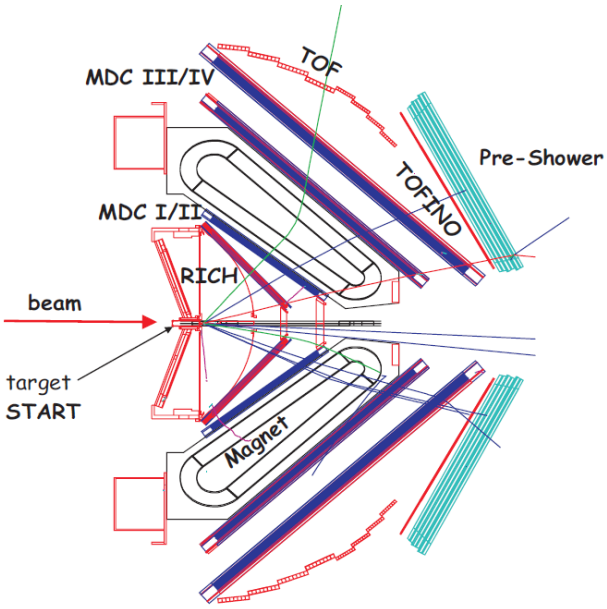

Figure 1. Schematic layout of the HADES detector in the configuration used for this experiment.

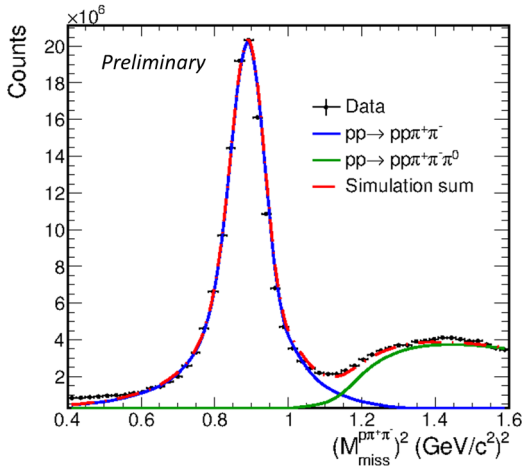

Figure 2. Squared missing mass distribution in the $pp \rightarrow pp\pi^+\pi^-$X reaction compared to simulations for the two pion production (blue) and three pion production (green). The total is shown as a red curve.

based on plastic scintillators covering polar angles, larger (TOF) and smaller (TOFINO) than 45°, respectively. For the analysis of the $pp \rightarrow pp\pi^+\pi^-$ reaction, the strategy is to select events with 3 prongs (one proton and two oppositely charged pions) and to apply a missing mass selection. In a first step, events with at least three tracks not correlated to RICH rings, one with a negative curvature, two with a positive curvature are selected. Particle identification of pions and protons is based on the correlation between momentum and time-of-flight. However, as no START detectors could be used in this experiment, only the information about the differences between time-of-flights was measured. To solve this problem, the negative track is used as a reference and is identified as a negative pion. Then, for each possible identification of positive tracks, *i.e.* π^+ or p, the time-of-flight differences with respect to the negative pion calculated using the reconstructed track length and the momentum are compared to the measured ones. The best combination is selected, by means of a χ^2 test taking into account errors on the time measurements.

The distribution of missing mass of the reaction $pp \rightarrow p\pi^+\pi^-X$ ($M_{miss}^{p\pi^+\pi^-}$) displays a clear peak corresponding to a missing proton (fig. 2). The structure at larger missing masses is mostly due to events with both a missing nucleon and a missing pion. This is corroborated by results of simulations for the reactions $pp \rightarrow pp\pi^+\pi^-$ and $pp \rightarrow pp\pi^+\pi^-\pi^0$, which, as shown in fig. 2 reproduces fairly well both structures. The missing mass distribution is weakly sensitive to the differential distributions in the model, which were taken assuming production according to the available phase space. But, it is important to note that the width of the proton peak in the missing mass distribution is very well reproduced by the simulation. This confirms that the modeling of the detector resolution adopted in the simulation and based on a parametrization of full scale GEANT simulations (see below) gives very realistic results. One can however notice an excess yield in the low missing mass tail, which is due to a small contamination of misidentified particles. To take into account both sources of background, the selection of the signal was performed in 25 bins of pπ^- invariant masses ($M_{p\pi^-}$) and 20 bins of cosine of the angle of the $p\pi^-$ pair in the center-of-mass ($\cos\theta_{p\pi^-}^{CM}$). For each bin, the three pion contribution was first subtracted based on the simulation. Then, the resulting missing mass distribution was fitted using the sum of two gaussians, representing the signal and of one polynomial for the background (fig. 4). This allowed to calculate the probability of an event to be a signal event, as a function of $M_{miss}^{p\pi^+\pi^-}$, $M_{p\pi^-}$, $\cos\theta_{p\pi^-}^{CM}$. The background subtracted differential distributions are then obtained by applying this probability as a weight to each event. In order to determine the geometrical acceptance and the reconstruction efficiency for each particle, detector hits produced by π^+, π^- and protons taking into account the experimental effects (detector geometry, energy loss, detector response,...) were produced using GEANT simulations and processed through the reconstruction and analysis code as for the real events. Acceptance and efficiency matrices were calculated as a function of the momentum, the polar and azimuthal angles in the laboratory [9]. The normalization of the experimental yield is obtained using the analysis of events produced in elastic scattering, as described in [10]. The final differential distributions are obtained after background subtraction, efficiency corrections and normalization as displayed in fig. 3. The error bars include statistical and uncorrelated systematic errors due to efficiency corrections and background subtraction. The differential cross sections are also affected by a global error of 7%, mainly due to the normalization uncertainty.

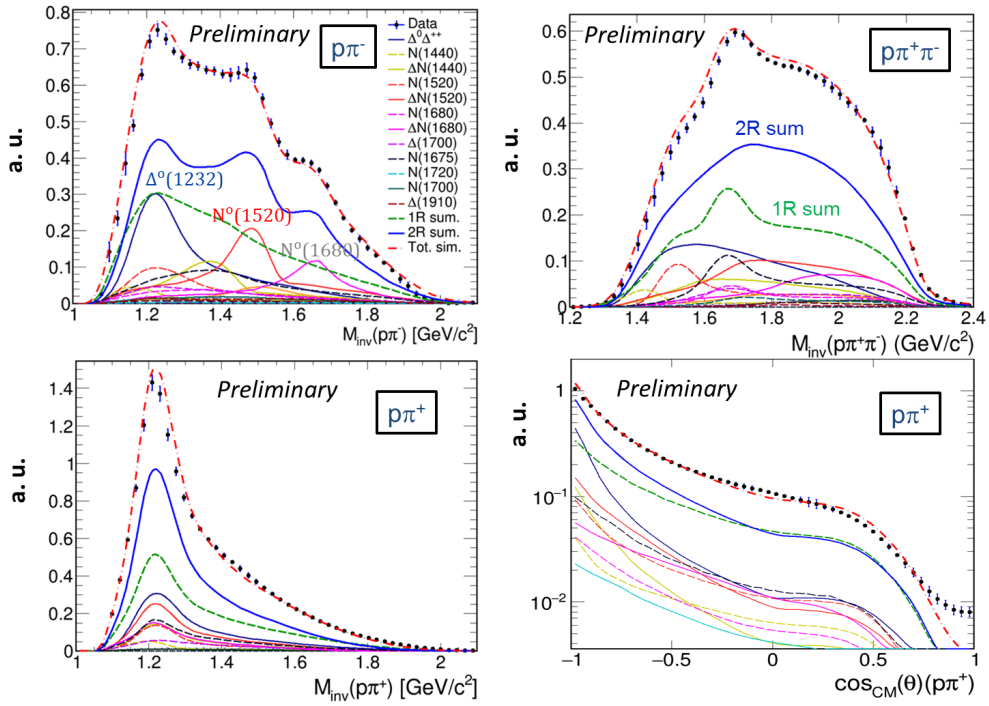

Figure 3. $p\pi^-$(top left), $p\pi^+\pi^-$(top right), $p\pi^+$ (bottom left) invariant masses and distribution of the center-of-mass angle of the $p\pi^+$ system. Data (black dots) are compared to the results of the fit with the resonance model (dashed red). The total double (blue) and single (dashed green) contributions are shown together with the most important individual contributions (see color code on the picture).

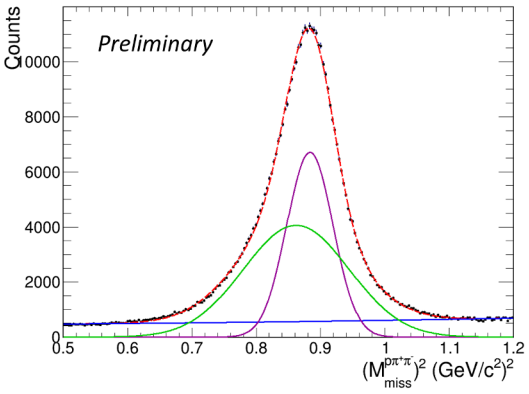

Figure 4. Squared missing mass distribution in the $pp \rightarrow pp\pi^+\pi^-$X reaction after subtraction of the three pion production contribution. The red curve represents the result of a fit with the sum of two Gaussians (violet and green curves) and of a polynomial (blue curve).

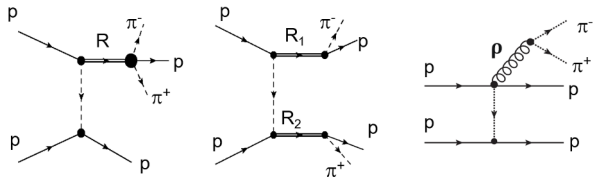

Figure 5. Diagrams of the three processes taken into account in the simulation of the $pp \rightarrow pp\pi^+\pi^-$ reaction. Left: Excitation of one positively charged resonance followed by decay into $p\pi^+\pi^-$. Center: Excitation of one doubled charged and one neutral resonance followed by their decay into $p\pi^-$ and $p\pi^+$ respectively. Right: direct ρ meson production.

3 HADES resonance model

To describe our data, we developed a model for the $pp \rightarrow pp\pi^+\pi^-$ reaction based on three different processes: the excitation of one resonance, with subsequent decay into a proton and two pions ($R \rightarrow p\pi^+\pi^-$) (fig. 5 Left), the excitation of two resonances decaying into a proton and a pion ($R_1, R_2 \rightarrow p\pi$) (fig. 5 Center) and the direct ρ production followed by its decay ($\rho \rightarrow \pi^+\pi^-$) (fig. 5 Right).

Useful constraints on the single resonance excitation in the pp reaction at 3.5 GeV are available thanks to previous data analyses of the HADES collaboration of respectively $NN\pi$ [10] and $pK\Lambda$ [11]. In [10], a model based on an incoherent sum of resonant contributions decaying in the πN channel has been used. Using a fit of the measured differential cross sections in the $pp\pi^0$ and $pn\pi^+$ channels, the cross sections for the excitation of various baryon resonances (Δ(1232), N(1440), N(1535), Δ(1700)) could be established (see table 1). However, for other baryons, due to the overlap with neighboring states, only upper limits for the cross sections could be extracted, as shown in table 1. The dependence of differential cross section on the four-momentum transfer, which, for fixed masses of the reaction products, is fully correlated to the angular distri-

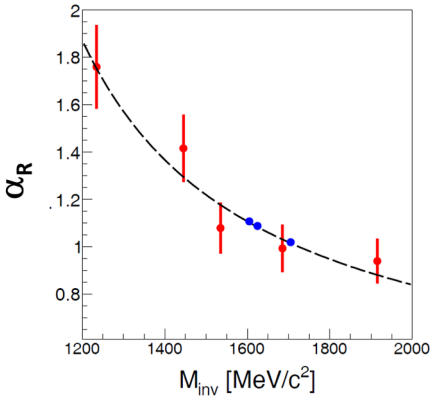

Figure 6. Dependency of the constant α_R used for the parametrization of the four-momentum transfer dependence of the cross section (Eq. 1) on the resonance mass M^R_{pole} obtained from fits to the data of 1π production analysis [10].

bution, was parametrized as

$$\frac{d\sigma}{dt} \sim t^{-\alpha_R}, \tag{1}$$

where t is the four momentum transfer $t = (p - p_R)^2$ at the resonance excitation vertex, calculated between the four-momentum vectors of the outgoing resonance (p_R) and the incoming nucleon (p). The parameter α_R could be fitted to the data and showed a decrease as a function of the mass of the resonance (see fig. 6).

Resonance	$\Gamma_{N\pi\pi}/\Gamma_{tot}(\%)$	σ_R [mb]
$N(1440)$	65	1.50 ± 0.37
$N(1520)$	55	1.8 ± 0.3
$N(1535)$	46	0.15 ± 0.05
$\Delta(1600)$	15	$< 0.24 \pm 0.10$
$\Delta(1620)$	25	$< 0.10 \pm 0.03$
$N(1650)$	45	$< 0.81 \pm 0.13$
$N(1675)$	45	$< 1.65 \pm 0.27$
$N(1680)$	65	$< 0.9 \pm 0.15$
$N(1720)$	20	$< 4.4 \pm 0.7$
$\Delta(1700)$	15	$< 0.45 \pm 0.16$
$\Delta(1905)$	15	$< 0.85 \pm 0.53$
$\Delta(1910)$	25	$< 0.38 \pm 0.16$

Table 1. Cross sections in units of mb for excitation of a positively charged resonance extracted from the one pion analysis [10].

Resonance	$\Gamma_{K\Lambda}/\Gamma_{tot}(\%)$	$\sigma(N^* \rightarrow pK\Lambda)[\mu b]$
$N^*(1650)$	7 ± 4	$8.6 \pm 0.6 \pm 2.1$
$N^*(1710)$	15 ± 10	$11.7 \pm 1.0 \pm 2.8$
$N^*(1720)$	4 ± 1	$2.4 \pm 1.3 \pm 0.4$
$N^*(1875)$	4 ± 2	$1.5 \pm 1.3 \pm 0.4$
$N^*(1880)$	2 ± 1	$14.9 \pm 0.2 \pm 3.6$

Table 2. Cross sections in units of μb for the single positively charged resonances extracted from $pp \rightarrow pK\Lambda$ analysis (third column) [11] . The ratio of $K\Lambda$ to total branching ratios derived from values in [12] is indicated in the second column.

In [11], a Partial Wave Analysis developed by the Bonn-Gatchina group was conducted for several data sets measured in the reaction $pp \rightarrow pK\Lambda$ at various energies. In this way, the amplitudes for excitation of five heavy resonances $(N^\star(1650), N^\star(1710), N^\star(1720), N^\star(1875), N^\star(1880))$ in the $pp \rightarrow pK\Lambda$ channel could be determined (see table 2).

Both results were used as starting inputs in our model for the single resonance contributions in the $pp\pi^+\pi^-$ channel. The decays into the different $N\pi\pi$ channels were taken into account, with $N\rho$ branching ratio from the preliminary results of a Bonn-Gatchina PWA analysis [13] and the total, $\Delta\pi$ and Nσ branching ratios consistent with [12] within errors. For the double resonance excitation, no experimental information is existing in our energy range. We took the branching ratios to Nπ from [14], as in [10] and for the angular distributions, we adapted the parametrization Eq.(1) to take into account the excitation of baryons R1 and R2 at the two vertices:

$$\frac{d\sigma}{dt} \sim t^{-0.5(\alpha_{R1}+\alpha_{R2})} \tag{2}$$

where α_{R1} and α_{R2} are the parameters determined for the single excitation of the two baryons. The direct ρ contribution was generated according to uniform phase space.

Following the approach of [10], the simulations of the resonance production and decay were performed with PLUTO++ [15], a simulation framework for heavy ion and hadronic reactions. The decay channels were added incoherently and filtered with the HADES acceptance matrices deduced from GEANT simulations, as mentioned above. The cross sections for the different contributions were determined from a fit of the four invariant mass distributions $M_{inv}(p,\pi^+)$, $M_{inv}(p,\pi^-)$, $M_{inv}(p,\pi^+,\pi^-)$ and $M_{inv}(\pi^+,\pi^-)$, based on a χ^2 minimization. Fig. 3 displays some examples of comparison of experimental distributions measured in the HADES acceptance with the fit results. Many different iterations have been performed, in order to check the robustness of the fitting procedure and to reduce the number of parameters. It can be observed that the cocktail describing the data results from several significant contributions, corresponding either to the single or to the double baryon excitation. For the double resonance excitation, which in the pp$\pi^+\pi^-$ exit channel, implies the excitation of a double charged Δ , preliminary results show that only the $\Delta(1232)^{++}$ is found to have a significant contribution. The associated neutral baryon is mostly a $\Delta(1232)^0$, but significant contributions from N(1440), N(1520), N(1535) and N(1680) are also found. The $\Delta(1232)^{++}$ is excited very copiously, either in association with another resonance or produced in the decay of a heavier baryon. The cross sections for the single resonance excitation are found to be compatible with the previous analyses [10, 11]. In addition, the new analysis allows to determine the cross sections for the single excitation of some resonances, for which only upper limits could be

provided previously. The results are also being compared to predictions of transport models. Most of the used models include double resonance excitation, but the cross sections are very scattered, even for the $\Delta(1232)^{++}\Delta(1232)^{0}$. Our data can therefore be used as constraints for the double resonance excitation, which is particularly important in view of the upcoming HADES and CBM experiments which will be performed at higher energies at the FAIR facility. In order to test the validity of adding incoherently

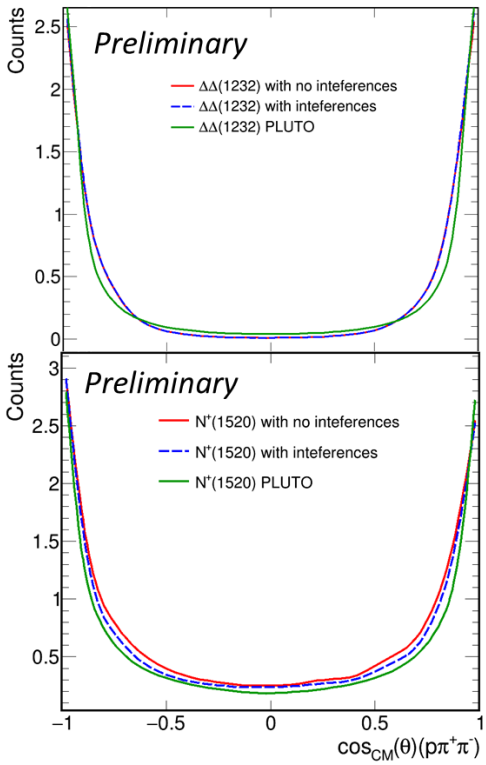

Figure 7. Comparison of the results of a Lagrangian model with (blue) and without (red) interferences between the different graphs. The simulations with the resonance model are shown in green. Top: Distribution of the $(p\pi^{+})$ centre of mass angular distribution for the double $\Delta^{++}(1232)$ contribution. Bottom: Distribution of the $(p\pi^{+}\pi^{-})$ centre of mass angular distribution for excitation of the $N^{+}(1520)$ decaying into $p\pi^{+}\pi^{-}$.

the cross sections of the different contributions in the resonance model, we developed a test Lagrangian model [16] for the main contributions, i.e. the double $\Delta(1232)$ and the N(1520) excitations. The values of coupling constants and cut-offs were taken as in [17]. The amplitudes of all contributing graphs, i.e. the direct, exchange, antisymmetrization graphs and for the N(1520) contribution, the decay into the various $\pi\pi N$ channels , i.e. $\Delta(1232)\pi$, ρN, $\sigma\pi$ was calculated. To evaluate the effect of the interferences, the calculation of the cross section from the squared sum of amplitudes was compared to an "incoherent" estimate deduced from the sum of squared amplitudes It was found that the effect of interferences was below 10% in all phase space regions (see fig. 7). In addition, it was interesting to observe that the angular distribution in the Lagrangian model is quite similar to the one due the parametrization of the four-momentum transfer dependence in our simple resonance model (see Eq. 1 and Eq. 2).

Dedicated models for the $pp \rightarrow pp\pi^{+}\pi^{-}$ [17, 18] can also be confronted to our data. The model of [17] is a Lagrangian model, based on meson exchange (π, σ, ρ, ω,...). It was developed for nucleon-nucleon reactions at incident energies below 2.2 GeV, and considers $\Delta(1232)^{++}\Delta(1232)^{0}$ as the only contributing double resonance excitation. In addition, it uses branching ratios from [14], which are in general, much larger than in [13]. The model of [18] uses experimental pion-nucleon amplitudes in a pion exchange approach and also considers one baryon exchange graphs. It is characterized by a strong contribution of double $\Delta(1232)$ excitation, hence producing a quite steep angular distribution, but also by a rather large yield coming from heavy resonances decaying to $p\pi^{+}\pi^{-}$.

4 ρ contribution

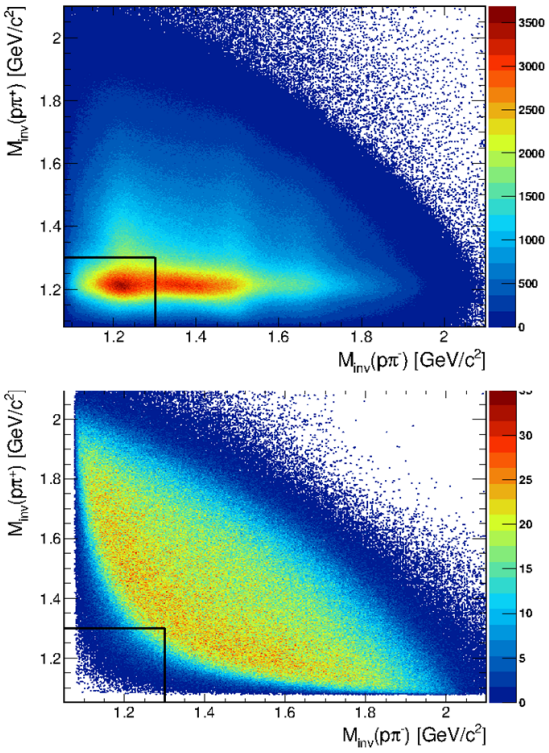

Figure 8. Correlation between $p\pi^{+}$ invariant mass and $p\pi^{-}$ invariant mass for data (top) and for simulation of the $pp \rightarrow pp\rho$ reaction (bottom). The black lines shows the first rejection ($M_{inv}(p\pi^{+}) < 1.3$ GeV/c^2 and $M_{inv}(p\pi^{-}) < 1.3$ GeV/c^2) applied to enhance the ρ signal.

The $\pi^{+}\pi^{-}$ channel is well suited to investigate the production of the ρ meson. However, the very large contribution from baryon resonances needs to be suppressed. To do so, cuts on the $p\pi$ invariant masses are first ap-

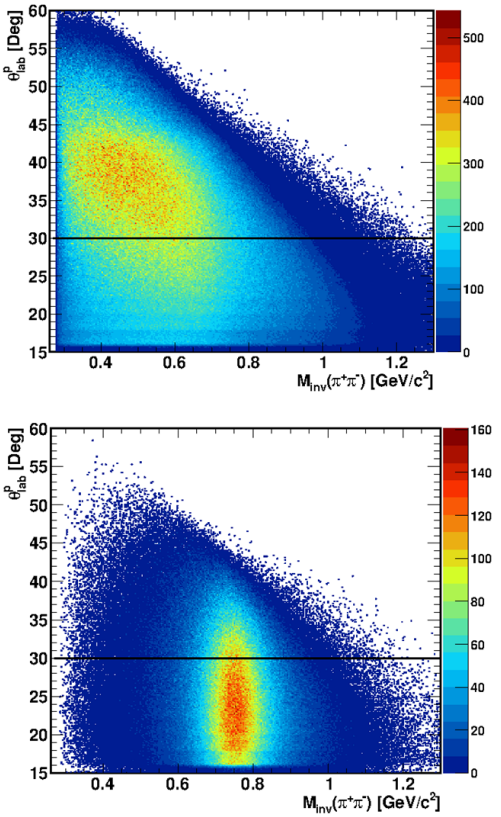

Figure 9. Correlation between the proton lab angle and the $\pi^+\pi^-$ invariant mass for data (top) and for simulation of the $pp \rightarrow pp\rho$ reaction (bottom). The black line shows the second rejection ($\theta_p > 30°$) applied to enhance the ρ signal.

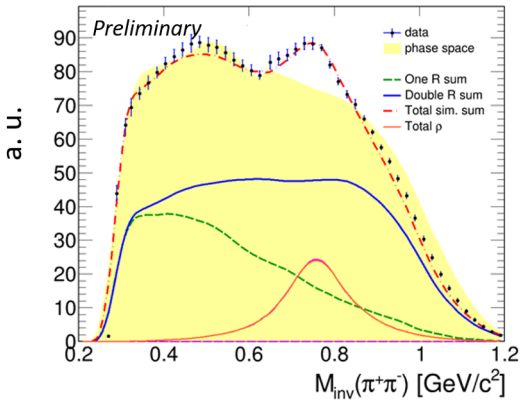

Figure 10. $\pi^+\pi^-$ invariant mass distribution after applying the kinematical rejections $M_{inv}(p\pi^+) < 1.3$ GeV/c^2, $M_{inv}(p\pi^-) < 1.3$ GeV/c^2 and $\theta_{lab}(p) < 30°$, compared to phase space (yellow area). The blue (respectively dashed green) curves represent the double (respectively single) resonance contribution from the resonance model (see text) and the red curve is the direct ρ contribution. The dashed red curve shows the total [19].

plied (fig. 8), which suppresses very efficiently the contribution of the $\Delta(1232)$ resonance, while affecting very weakly the ρ production. Then, an additional threshold on the proton angle is applied to suppress protons emitted backwards in the center-of-mass which still mostly come from baryon resonance production (fig. 9). After both rejection criteria, a structure in the $\pi^+\pi^-$ invariant mass distribution appears around the ρ meson mass (see fig. **??**). The production of the ρ meson via baryon resonance decay is included in our simulation with branching ratios from the recent Bonn-Gatchina PWA. The corresponding ρ meson spectral function is significantly distorted from a Breit-Wigner, due to the coupling to the light baryons (e.g. N(1520)) which favors ρ mesons in the low mass tail. The observed excess with respect to the resonant contribution can be considered as due to the direct ρ production (see fig. 5 Right). Its yield can be extracted in bins of $\pi^+\pi^-$ angle. Preliminary results show a significant enhancement for forward/backward emission, which is consistent with the dominance of nucleon currents in the $pp \rightarrow pp\rho$ reaction, as also observed by DISTO [20]. Despite the model dependency, this analysis gives information on the ρ production mechanism and the role of baryon resonances in it. To enable a more direct comparison to data, the usual method for extracting the ρ production cross section based on a simple Breit-Wigner fit was also applied, although it suppresses the contribution due to the light baryons. The analysis is in progress and results on the cross section of the ρ meson production are expected soon.

5 Conclusion

These preliminary results show the interest of the $pp \rightarrow pp\pi^+\pi^-$ reaction to constrain in a quantitative way the baryon resonance contribution and the ρ meson production, which are important sources of e^+e^- pairs. The two contributions are strongly coupled due to the possible decay of baryon resonances in the ρN channel. In addition, according to the Vector Meson Dominance, it is expected that the electromagnetic coupling to baryons is fully mediated by the vector mesons. These data provide important information on nucleon-nucleon reaction mechanisms in general and constitute in particular important constraints for the models used for dielectron production, which will be essential in the context of the future experiments at FAIR with the HADES and CBM set-ups, at similar incident energy per nucleon than the present experiment.

6 Acknowledgements

SIP JUC Cracow, Cracow (Poland), National Science Center, 2016/23/P/ST2/040 POLONEZ, 2017/25/N/ST2/00580, 2017/26/M/ST2/00600; TU Darmstadt, Darmstadt (Germany), VH-NG-823, DFG GRK 2128, DFG CRC-TR 211, BMBF:05P18RDFC1; Goethe-University, Frankfurt (Germany) and TU Darmstadt, Darmstadt (Germany), ExtreMe Matter Institute EMMI at GSI Darmstadt; TU München, Garching (Germany), MLL München, DFG EClust 153, GSI TMLRG1316F, BmBF 05P15WOFCA, SFB 1258, DFG

FAB898/2-2; NRNU MEPhI Moscow, Moscow (Russia), in framework of Russian Academic Excellence Project 02.a03.21.0005, Ministry of Science and Education of the Russian Federation 3.3380.2017/4.6; JLU Giessen, Giessen (Germany), BMBF:05P12RGGHM; IPN Orsay, Orsay Cedex (France), CNRS/IN2P3; NPI CAS, Rez, Rez (Czech Republic), MSMT LM2015049, OP VVV CZ.02.1.01/0.0/0.0/16 013/0001677, LTT17003.

References

[1] G. Agakichiev et al. (HADES), Eur. Phys. J. **A41**, 243 (2009), 0902.3478
[2] P. Salabura *et al.* (HADES), *Exploring time like transitions in pp, $\pi^- p$ and heavy ion reactions with HADES*, NSTAR2019
[3] J.J. Sakurai, Phys. Rev. Lett. **22**, 981 (1969)
[4] G. Agakishiev et al. (HADES), Eur. Phys. J. **A48**, 74 (2012), 1203.1333
[5] G. Agakishiev et al. (HADES), Eur. Phys. J. **51**, 137 (2015)
[6] G. Agakishiev et al., Eur. Phys. J. **A50**, 82 (2014), 1403.3054
[7] G. Agakishiev et al. (HADES), Phys. Lett. **B742**, 242 (2015), 1410.8188
[8] G. Agakishiev et al., Phys. Lett. **B750**, 184 (2015), 1503.04013
[9] A. Belounnas (HADES), PoS **Hadron2017**, 213 (2018)
[10] G.. Agakishiev et al. (HADES), Eur. Phys. J. **A50**, 82 (2014), 1403.3054
[11] R. Münzer et al., Phys. Lett. **B785**, 574 (2018), 1703.01978
[12] M. Tanabashi et al. (Particle Data Group), Phys. Rev. D **98**, 030001 (2018)
[13] V.V. Sarantsev, private communication
[14] K. Nakamura et al. (Particle Data Group), J. Phys. G **37**, 075021 (2010)
[15] I. Fröhlich et al., PoS **ACAT2007**, 076 (2007), 0708.2382
[16] Van de Wiele, J., private communication
[17] X. Cao, B.S. Zou, H.S. Xu, Phys.Rev. **C81**, 065201 (2010), 1004.0140
[18] A.P. Jerusalimov, A.V. Belyaev, V.P. Ladygin, A.K. Kurilkin, A.Yu. Troyan, Yu.A. Troyan, Eur. Phys. J. **A51**, 83 (2015)
[19] A. Belounnas (HADES), EPJ Web Conf. **199**, 02012 (2019)
[20] F. Balestra et al. (DISTO), Phys. Rev. Lett. **89**, 092001 (2002), hep-ex/0209004